

# Development and implementation of plasma sprayed nanostructured ceramic coatings

M. Gell<sup>a,\*</sup>, E.H. Jordan<sup>b</sup>, Y.H. Sohn<sup>a,1</sup>, D. Goberman<sup>a</sup>, L. Shaw<sup>a</sup>, T.D. Xiao<sup>c</sup>

<sup>a</sup>Department of Metallurgy and Materials Engineering, University of Connecticut, U 136, 97 North Eagleville Road, Storrs, CT 06269, USA

<sup>b</sup>Department of Mechanical Engineering, University of Connecticut, Storrs, CT 06269, USA

<sup>c</sup>Inframat Corporation, 20 Washington Avenue, North Haven, CT 06473-2342, USA

## Abstract

A broad overview of the science and technology leading to the development and implementation of the first plasma sprayed nanostructured coating is described in this paper. Nanostructured alumina and titania powders were blended and reconstituted to a sprayable size. Thermal spray process diagnostics, modeling and Taguchi design of experiments were used to define the optimum plasma spray conditions to produce nanostructured alumina–titania coatings. It was found that the microstructure and properties of these coatings could be related to a critical process spray parameter (CPSP), defined as the gun power divided by the primary gas flow rate. Optimum properties were determined at intermediate values of CPSP. These conditions produce limited melting of the powder and retained nanostructure in the coatings. A broad range of mechanical properties of the nanostructured alumina–titania coatings was evaluated and compared to the Metco 130 commercial baseline. It was found that the nanostructured alumina–titania coatings exhibited superior wear resistance, adhesion, toughness and spallation resistance. The technology for plasma spraying these nanostructured coatings was transferred to the US Navy and one of their approved coating suppliers. They confirmed the superior properties of the nanostructured alumina–titania coatings and qualified them for use in a number of shipboard and submarine applications. © 2001 Elsevier Science B.V. All rights reserved.

**Keywords:** Nanostructured coatings; Wear resistant coatings; Plasma spray; Microstructure; Multi-disciplinary engineering; Technology

## 1. Introduction

The objective of this research was to develop and implement cost-effective plasma sprayed nanostructured ceramic coatings, with superior resistance to wear, erosion, cracking and spallation [1–5]. These attractive properties associated with a nanostructure (a grain size smaller than 100 nm) have been previously documented for bulk materials [6–13]. In this paper, a broad overview of the processing, characterization and testing leading to the development and implementation of the first nanostructured coating is described. With the large

number of applications in the US Navy, this program provided a ‘market pull’ for this new technology.

## 2. Processing: reconstituted nanostructured powders and plasma spray

The overall processing sequence for the plasma sprayed nanostructured Al<sub>2</sub>O<sub>3</sub>–13 wt.% TiO<sub>2</sub> coatings is illustrated in Fig. 1. Commercially available nanostructured powders of Al<sub>2</sub>O<sub>3</sub> and TiO<sub>2</sub>, obtained from Nanophase Technology Corporation™, Burr Ridge, IL, were mixed and reconstituted into plasma sprayable size agglomerates. Using Taguchi design of experiments, large, smooth and relatively dense nanostructured powders were reconstituted with minimum grain growth [1]. The reconstitution process consists of spray drying the slurry that contains nano-particles of appropriate proportion, and subsequent heat treatment at high temper-

\* Corresponding author. Tel.: +1-860-486-3514; fax: +1-860-486-4745.

E-mail address: mgell@mail.ims.uconn.edu (M. Gell).

<sup>1</sup> Now with Advanced Materials Processing and Analysis Center, Mechanical, Materials and Aerospace Engineering, University of Central Florida, Orlando, FL, USA.

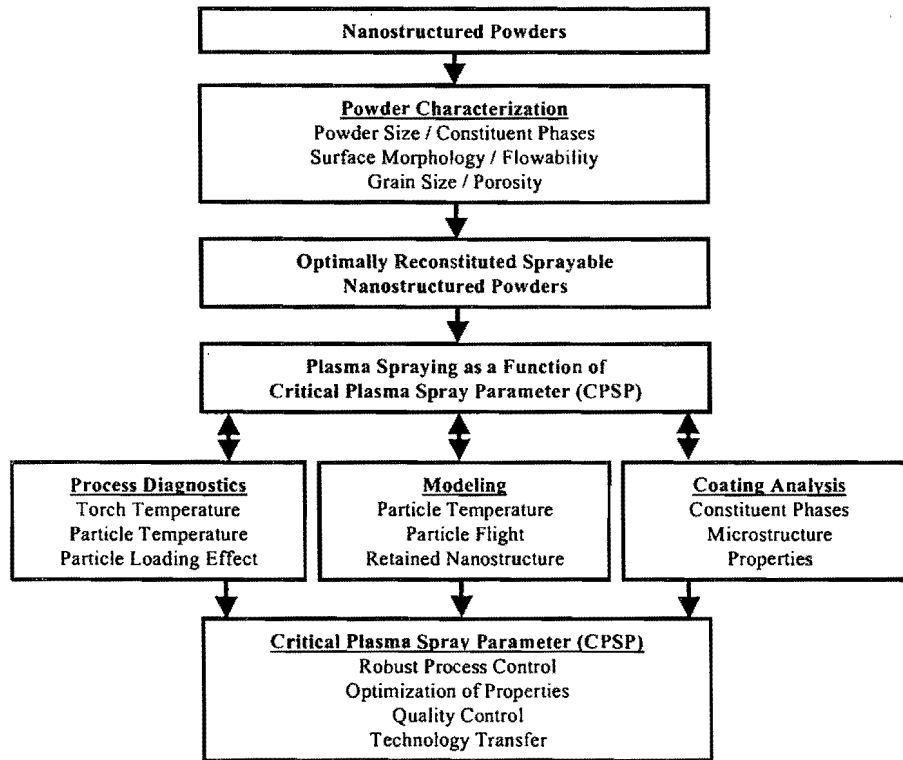


Fig. 1. Flow chart illustrating the processing and evaluation sequence for plasma sprayed nanostructured ceramic coatings.

ature (800–1200°C). The resultant  $\text{Al}_2\text{O}_3$ -13 wt.%  $\text{TiO}_2$  powders are hereafter denoted as unmodified. In addition, small amounts of other oxides were mixed to further enhance the properties of these nanostructure-derived coatings (hereafter denoted as modified nano-coating). The reconstitution process for modified agglomerates involved an additional step of plasma reprocessing, during which the modified powders were plasma heat-treated and air-quenched in a collection chamber. The reconstituted nanostructured powders were characterized extensively for the size, shape, morphology, phase constituents and composition. For comparison purposes, a commercially available powder (Metco-130) with the  $\text{Al}_2\text{O}_3$ -13 wt.%  $\text{TiO}_2$  composition was examined.

Fig. 2 shows the cross-sectional backscattered electron micrographs of Metco-130 and reconstituted, unmodified and modified nano-powders. Using X-ray diffraction (XRD) and scanning/transmission electron microscopy (SEM and TEM) equipped with energy dispersive spectroscopy (EDS), the phase constituents and their compositions were identified for these powders [1–4]. The  $\text{Al}_2\text{O}_3$  took the form of  $\alpha$ - $\text{Al}_2\text{O}_3$  for all the powders (dark regions in Fig. 2), while the  $\text{TiO}_2$  was in the form of anatase- $\text{TiO}_2$  for the Metco 130 powders and rutile- $\text{TiO}_2$  for unmodified powders.  $\text{TiO}_2$  was dissolved in oxide additives for the modified powders (light regions in Fig. 2). Previous work, using XRD line broadening

techniques, has shown that the grain size of anatase- $\text{TiO}_2$  was below 100 nm, while grain size of  $\alpha$ - $\text{Al}_2\text{O}_3$  and rutile- $\text{TiO}_2$  is greater than 100 nm [1]. The particle size estimated by Saltykov analysis and MicroTack™ measurements ranged from 15 to 150  $\mu\text{m}$  for all powders with an average value of approximately 50  $\mu\text{m}$  [4]. Fig. 2 also shows that the commercial Metco 130 powders are dense while the reconstituted nanopowders contain up to 45% porosity.

In order to control the plasma spray process, extensive spray trials were carried out to investigate the effects of a wide range of processing variables on the microstructure and properties of the nanostructured alumina-titania coatings. Several processing parameters of the plasma spray such as: carrier gas flow rate; spray distance; flow rate ratio of Ar to  $\text{H}_2$ ; powder feed rate; and gun speed, were held constant during this investigation. It was found that the microstructure and properties could be related to an empirical parameter that is defined as the critical plasma spray parameter, CPSP [Eq. (1)]:

$$\text{CPSP} = \frac{\text{voltage} \cdot \text{current}}{\text{primary gas (Ar) flow rate}} \quad (1)$$

CPSP can be directly related to the plasma torch/particle temperature, which was measured by two-color pyrometer [14]. Using various CPSP, alumina-titania coatings were plasma sprayed and the resulting microstructure and properties were evaluated. In addition,

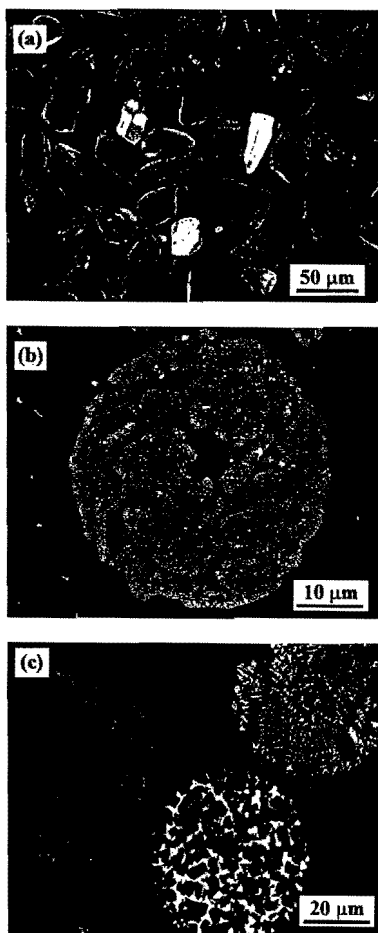


Fig. 2. Backscattered electron micrographs of (a) Metco-130 powders and reconstituted (b)  $\text{Al}_2\text{O}_3$ -13 wt.%  $\text{TiO}_2$  without the additives and (c)  $\text{Al}_2\text{O}_3$ -13 wt.%  $\text{TiO}_2$  with the additives.

CPSP was employed in computational fluid dynamics analyses [15] to validate the experimental results and to optimize coating deposition.

### 3. Phase constituents and microstructure of nanostructured coatings

All coatings, Metco-130, unmodified and modified alumina-titania coatings, consisted of  $\gamma\text{-Al}_2\text{O}_3$  and  $\alpha\text{-Al}_2\text{O}_3$  [2–4].  $\text{TiO}_2$  was found to be in solid solution with  $\gamma\text{-Al}_2\text{O}_3$  [2–4,7,16]. Fig. 3 shows the volume percent of  $\gamma\text{-Al}_2\text{O}_3$  determined by quantitative X-ray diffraction [4] as a function of CPSP, and, in turn, a function of plasma torch/particle temperature [14]. The volume percent of  $\gamma\text{-Al}_2\text{O}_3$  increases with increasing CPSP for coatings plasma sprayed with reconstituted nanostructured powders up to  $\text{CPSP}=390$ . The volume percent of  $\gamma\text{-Al}_2\text{O}_3$  for the Metco-130 coatings remains unchanged as a function of CPSP up to  $\text{CPSP}=390$ . But, all coatings show a slight decrease in the percent

of  $\gamma\text{-Al}_2\text{O}_3$  at  $\text{CPSP}=410$ . These variations in the phase constituents as a function of CPSP can be explained based on the starting powder morphology and the plasma spray process (i.e. melting and splat quenching) [2–4]. Metco 130 coatings were sprayed using dense (i.e. high thermal conductivity)  $\alpha\text{-Al}_2\text{O}_3$  powder. This powder melts in the torch and is splat-quenched to form metastable  $\gamma\text{-Al}_2\text{O}_3$  in the coating [17–20]. However, for porous reconstituted nanostructured powders with lower thermal conductivity, the amount of  $\gamma\text{-Al}_2\text{O}_3$  increased with CPSP up to 390. This observation indicates that the nano-powder agglomerates are partially melted and retain  $\alpha\text{-Al}_2\text{O}_3$  from the powder in the coating [2–4]. The increase in the amount of  $\alpha\text{-Al}_2\text{O}_3$  at  $\text{CPSP}=410$  can be attributed to a solid phase transformation ( $\gamma \rightarrow \alpha$ ) that occurs after rapid solidification as a result of substrate heating [4,17–20].

The results from the quantitative XRD on the phase constituents were confirmed by electron microscopy (SEM/EDS and TEM) [2–4]. While the Metco 130 coatings exhibited splat-quenched single phase ( $\gamma\text{-Al}_2\text{O}_3$ ) microstructure, plasma sprayed alumina-titania coatings from the reconstituted nano-powders exhibited a bimodal microstructure. An example of the bimodal microstructure of the plasma sprayed modified alumina-titania coating is shown in Fig. 4. Region 'F' corresponds to fully melted and splat-quenched regions ( $\gamma\text{-Al}_2\text{O}_3$  supersaturated with  $\text{Ti}^{4+}$ ) while region 'P' corresponds to a partially melted region where the initial microstructure of the reconstituted nanostructured agglomerates is retained. The partially melted region consists of  $\alpha\text{-Al}_2\text{O}_3$  particles (black; less than  $1 \mu\text{m}$  in size) embedded in  $\gamma\text{-Al}_2\text{O}_3$  (white) supersaturated with

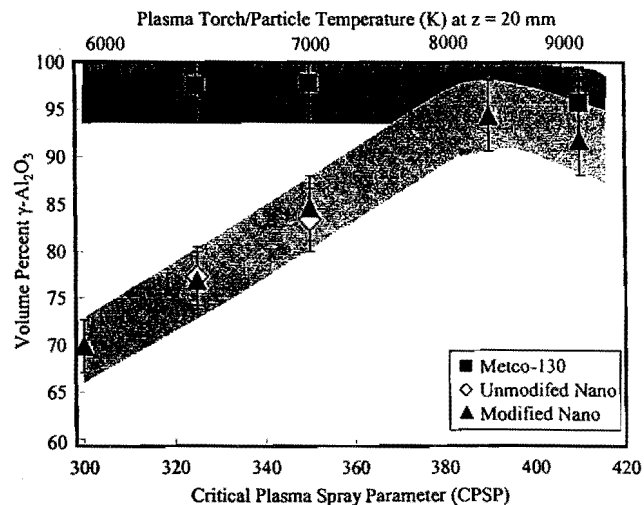


Fig. 3. Volume percent of  $\gamma\text{-Al}_2\text{O}_3$  in  $\text{Al}_2\text{O}_3$ -13 wt.%  $\text{TiO}_2$  coatings as a function of CPSP, measured using X-ray diffraction patterns with external standards. The plasma torch/particle temperature can be directly related to CPSP.

Ti<sup>4+</sup> as presented in Fig. 4b. The presence of Ti in  $\gamma$ -Al<sub>2</sub>O<sub>3</sub> (i.e. supersaturated with Ti<sup>4+</sup> in  $\gamma$ -Al<sub>2</sub>O<sub>3</sub>) was observed from EDS. The modified nanostructured coatings were similar in microstructure with slightly larger  $\alpha$ -Al<sub>2</sub>O<sub>3</sub> particulates (0.5–3  $\mu$ m). This unique, bimodal microstructure is only obtained by plasma spray of reconstituted nanostructured powders [2–4].

Extensive transmission microscopy [4] also confirmed the bimodal microstructure. While coatings plasma sprayed from Metco 130 powders contain mostly  $\gamma$ -Al<sub>2</sub>O<sub>3</sub>, the coatings plasma sprayed with reconstituted nanostructured powders contained both splat-quenched  $\gamma$ -Al<sub>2</sub>O<sub>3</sub> and retained  $\alpha$ -Al<sub>2</sub>O<sub>3</sub>. It was also found that the grain size of the splat-quenched  $\gamma$ -Al<sub>2</sub>O<sub>3</sub> was extremely small (20–70 nm) while that of the  $\alpha$ -Al<sub>2</sub>O<sub>3</sub> was approximately 0.5–3  $\mu$ m. Fig. 4c,d shows the microstructure of plasma sprayed nanostructured coating (unmodified) that includes nano-grained  $\gamma$ -Al<sub>2</sub>O<sub>3</sub> and submicron/micron-grained  $\alpha$ -Al<sub>2</sub>O<sub>3</sub>.

Based on quantitative image analysis, the two regions of the microstructure were examined as a function of CPSP, as presented in Fig. 5. The fraction of the coating microstructure, represented by region 'P' decreases with increasing CPSP and the corresponding increase in plasma torch/particle temperature. Near-complete melting followed by splat quenching was observed at relatively high CPSP, corresponding to increase in the microstructural region 'F' with increasing CPSP. Therefore, it can be concluded that splats, which formed through melting the feed powder and rapid solidification,

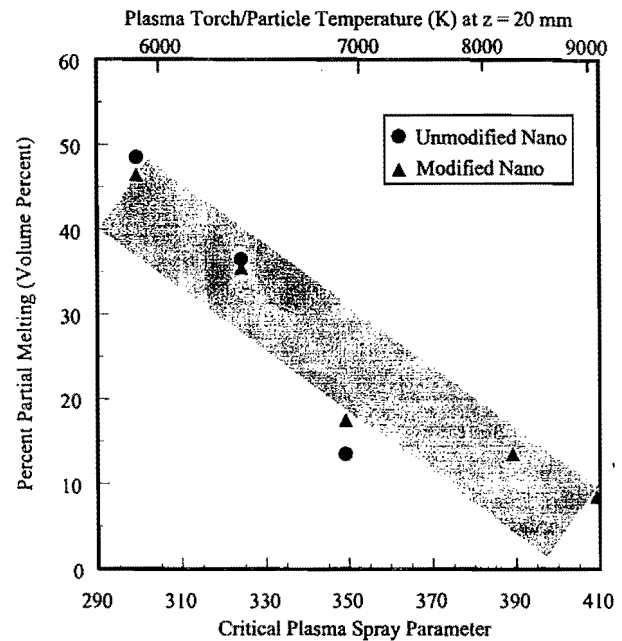


Fig. 5. Percentage of coating that is partially melted, determined by quantitative image analysis as a function of CPSP.

consisted of nanometer-sized  $\gamma$ -Al<sub>2</sub>O<sub>3</sub>, whereas the particulate microstructure, which was formed via partial melting and liquid phase sintering, consisted of submicrometer-sized  $\alpha$ -Al<sub>2</sub>O<sub>3</sub> with small amounts of nanometer-sized  $\gamma$ -Al<sub>2</sub>O<sub>3</sub>. Furthermore, the bimodal

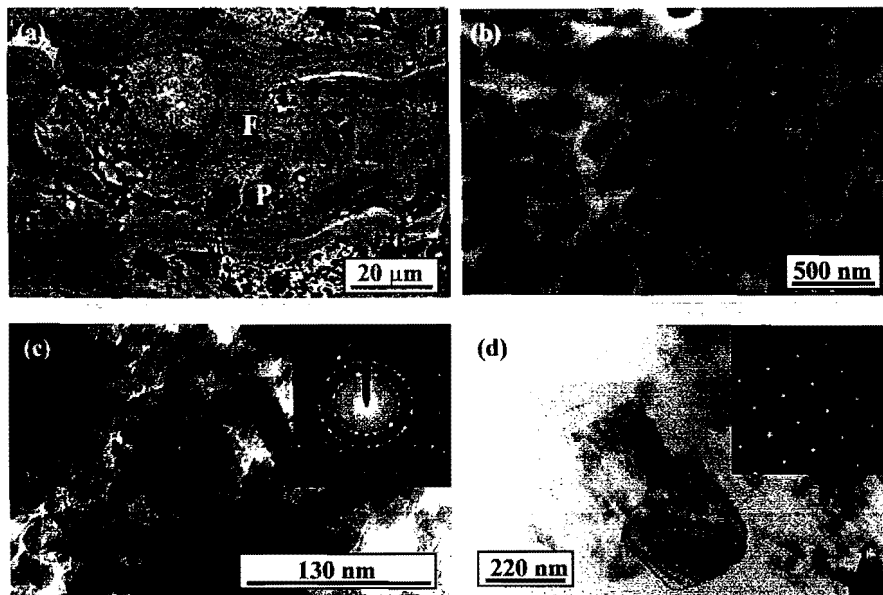


Fig. 4. Electron micrographs from plasma sprayed nanostructured Al<sub>2</sub>O<sub>3</sub>-13 wt.% TiO<sub>2</sub> coatings. (a) The coating consists of two regions identified by 'F', fully melted and splat-quenched  $\gamma$ -Al<sub>2</sub>O<sub>3</sub> region and 'P', partially melted region where the microstructure of the starting agglomerate is retained. (b) The partially melted region 'P' consists of  $\alpha$ -Al<sub>2</sub>O<sub>3</sub> (black) embedded in  $\gamma$ -Al<sub>2</sub>O<sub>3</sub> (white). The transmission electron micrographs (TEM) from the partially melted region 'P' shows the (c) small  $\gamma$ -Al<sub>2</sub>O<sub>3</sub> grains and (d) relatively larger  $\alpha$ -Al<sub>2</sub>O<sub>3</sub> grains.

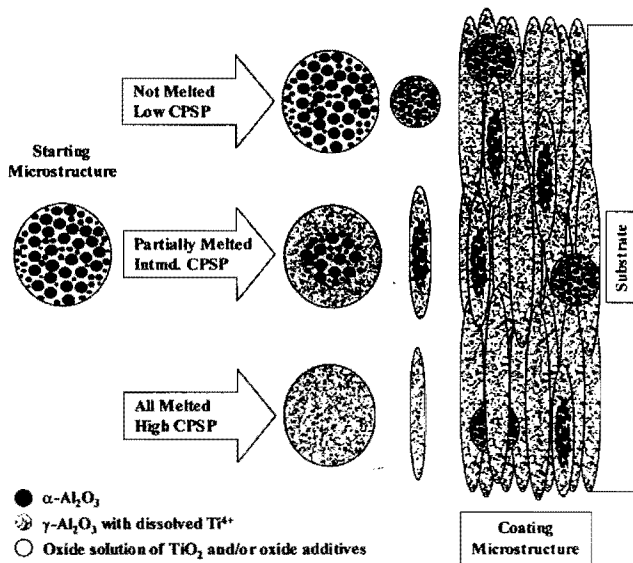


Fig. 6. A schematic illustration of phase transformations and microstructural development during the plasma spray deposition of reconstituted nanostructured  $\text{Al}_2\text{O}_3$ -13 wt.%  $\text{TiO}_2$  agglomerates.

distribution of the microstructure in nanostructured coatings can be controlled by CPSP [2–4]. The phase transformations during the plasma spray deposition of reconstituted alumina–titania, as a function of CPSP, can be summarized as shown in Fig. 6 [4].

#### 4. Properties of nanostructured coatings

Physical and mechanical properties of the plasma sprayed coatings including: density; hardness; indentation crack resistance; adhesion strength; spallation resistance in bend and cup-tests; and resistance to abrasive and sliding wear, were evaluated as a function of CPSP [2,3]. In all tests, coatings with bimodal microstructures made from nanostructured powders showed unique and superior properties. Specifically, significant improvement in indentation crack resistance, spallation resistance and wear resistance was consistently observed. Typical results from cup and bend tests are presented in Figs. 7

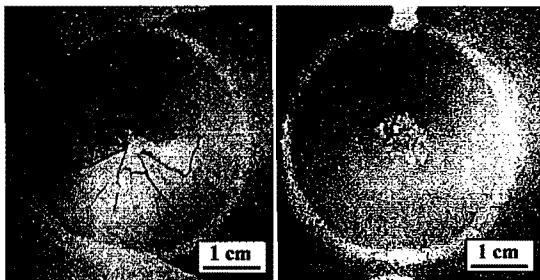


Fig. 7. Typical results observed for plasma sprayed  $\text{Al}_2\text{O}_3$ -13 wt.%  $\text{TiO}_2$ : (a) Metco 130 coatings; and (b) reconstituted nanostructured coatings (CPSP=350) containing a bimodal microstructure.

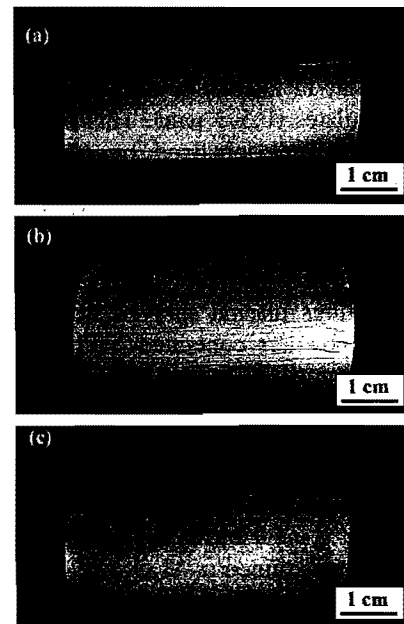


Fig. 8. Representative results from bend tests: (a) complete spallation for Metco 130 coatings; (b) partial; and (c) minimum spallation for reconstituted nanostructured coatings (CPSP=325) containing a bimodal microstructure.

and 8, respectively. While significant spallation is observed for Metco-130 coatings, nanostructured  $\text{Al}_2\text{O}_3$ -13 wt.%  $\text{TiO}_2$  coatings exhibit minor damage.

This drastic improvement in cracking can be understood from the results of indentation tests performed on these coatings. At selected CPSPs, improved crack resistance, defined as reciprocal of the crack length, was observed for coatings plasma sprayed from reconstituted  $\text{Al}_2\text{O}_3$ -13 wt.%  $\text{TiO}_2$  as shown in Fig. 9. In Metco-130, long and well-defined splat boundaries provide easy crack propagation paths. In the nanostructured alumina–

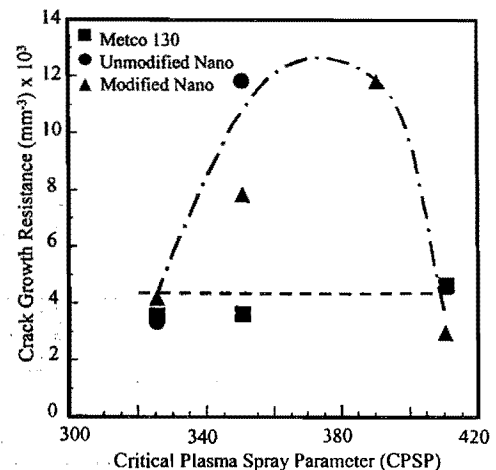


Fig. 9. Indentation crack resistance of plasma sprayed  $\text{Al}_2\text{O}_3$ -13 wt.%  $\text{TiO}_2$  coatings as a function of CPSP.

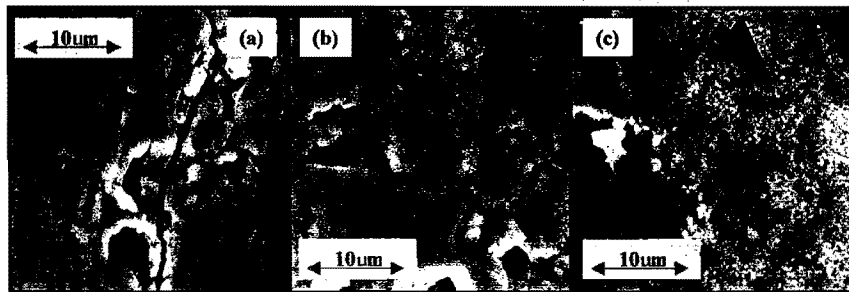


Fig. 10. Indentation cracks observed for (a) Metco-130 and (b,c) nanostructured alumina–titania coatings. (a) Long, wide cracks along the splat boundaries were observed for Metco-130 coatings; (b,c) short, narrow cracks arrested at partially melted regions (arrow) were observed for nanostructured alumina–titania coatings.

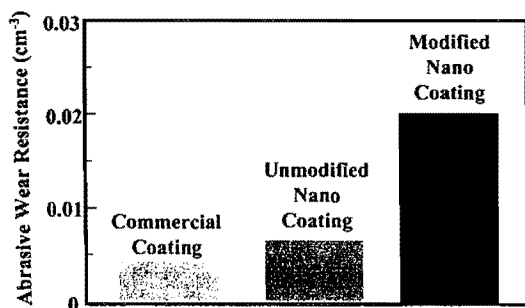


Fig. 11. Abrasive wear resistance of plasma sprayed Al<sub>2</sub>O<sub>3</sub>-13 wt.% TiO<sub>2</sub> coatings at CPSP=350.

titania coatings with a bimodal microstructure, the splat-boundary structure is periodically disrupted by regions of partially melted powders. Cracks propagating through splat boundaries are arrested and/or deflected after encountering the partially melted regions in the coating as presented in Fig. 10.

A significant improvement in the abrasive wear resistance was observed [5] as highlighted in Fig. 11, especially for the modified nanostructured coatings. This improvement can be visually confirmed from the wear and scratched surfaces presented in Fig. 12, where a large scale cracking/material removal occurs for Metco-

130 and reduced material removal without cracking occurs for the reconstituted nanostructured coatings.

### 5. Implementation of plasma sprayed nanostructured coatings

The technology for plasma spraying the nanostructured coatings was transferred to the US Navy and one of their approved coating suppliers. From independent tests carried out at the US Navy as well as at the coating supplier, superior properties of the nanostructured Al<sub>2</sub>O<sub>3</sub>-13 wt.% TiO<sub>2</sub> coatings were consistently confirmed. The modified nanostructured alumina–titania coatings have been qualified for use in a number of shipboard and submarine applications such as: arm weldment; bulkhead pivot arm; bearing sled; front and aft door support; magnet arm; sockets and arm pivot pins; periscope guides; hydraulic piston; and reduction gear set. The successful and efficient technology transfer was carried out by the use of CPSP and process diagnostic tools. The relationship between the plasma torch temperature and CPSP in a pre-specified industrial setting (i.e. different plasma systems, torches, etc.) was quickly established by process diagnostics. Then, an optimum CPSP for the coating supplier was defined to

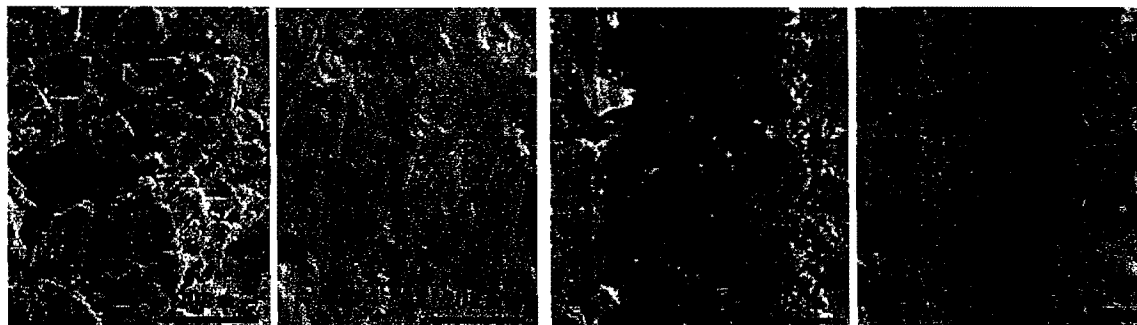


Fig. 12. Surface morphology of (a,c) Metco-130 and (b,d) reconstituted nanostructured Al<sub>2</sub>O<sub>3</sub>-13 wt.% TiO<sub>2</sub> coatings after the (a,b) abrasive wear and (c,d) scratch test (courtesy of Dr T.E. Fischer).

deposit nanostructured coatings with a partially melted microstructure.

## 6. Summary

A broad overview of the science and technology leading to the development and implementation of the first nanostructured coating with superior properties was presented. The use of a critical plasma spray parameter (CPSP) permitted an efficient integration of multi-disciplinary engineering efforts to produce nanostructured  $\text{Al}_2\text{O}_3$ -13 wt.%  $\text{TiO}_2$  coatings that are unique in microstructure, superior in properties and readily technology transferable. The key to the improved properties is the production of a bimodal microstructure, which imparts improved toughness to the coating. The nanostructured  $\text{Al}_2\text{O}_3$ -13 wt.%  $\text{TiO}_2$  coatings have been approved by the U.S. Navy for shipboard and submarine applications.

## Acknowledgements

We appreciate the vision and dedication of Dr Lawrence Kabacoff, the Program Manager of ONR Contract #N00014-98-C-0010, that provided the 'market-pull' for this emerging technology.

## References

- [1] L. Shaw, D. Goberman, R. Ren et al., *Surf. Coat. Technol.* 130 (2000) 1.
- [2] E.H. Jordan, M. Gell, Y.H. Sohn et al., *Mater. Sci. Eng. A* 301 (2001) 80.
- [3] M. Gell, E.H. Jordan, Y.H. Sohn, D. Goberman, L. Shaw, T.L. Bergman, B. Cetegen, S. Jiang, M. Wang, T.D. Xiao, Y. Wang, P.R. Strutt, *Mater. Process. Technol.*, in press.
- [4] D. Goberman, Y.H. Sohn, L. Shaw, E.H. Jordan, M. Gell, *Acta Mater.*, submitted for publication.
- [5] Y. Wang, S. Jiang, M. Wang, S. Wang, T.D. Xiao, P.R. Strutt, *Wear* 237 (2000) 176.
- [6] H. Gleiter, *Nanostruct. Mater.* 1 (1992) 1.
- [7] H. Hahn, *Nanostruct. Mater.* 2 (1993) 251.
- [8] R.W. Siegel, *Nanophase materials: synthesis, structure and properties*, in: F.E. Fujita (Ed.), *Physics of New Materials*, Springer, Heidelberg, 1992.
- [9] R.S. Mishra, C.E. Leshner, A.K. Mukherjee, *Mater. Sci. Forum* 225–227 (1996) 617.
- [10] R.W. Siegel, *Mater. Sci. Forum* 235–238 (1997) 851.
- [11] K. Jia, T.E. Fischer, *Wear* 200 (1996) 206.
- [12] K. Jia, T.E. Fischer, *Wear* 203–204 (1997) 310.
- [13] B. Kear, L.E. Cross, J.E. Keem et al., *Research Opportunities for Materials with Ultrafine Microstructure*, National Materials Advisory Board, National Academy Press, Washington D.C., 1989, Committee on Materials with Submicron-Sized Microstructure.
- [14] B.M. Cetegen, W. Yu, *J. Thermal Spray Technol.* 8 (1999) 57.
- [15] I. Ahmed, T.L. Bergman, *J. Thermal Spray Technol.* 9 (2000) 215.
- [16] B.H. Kear, Z. Kalman, R.K. Sadangi, G. Skandan, J. Colaizzi, W.E. Mayo, *J. Thermal Spray Technol.* 9 (2000) 483.
- [17] R. McPherson, *J. Mater. Sci.* 15 (1980) 3141.
- [18] R. McPherson, *J. Mater. Sci.* 8 (1973) 851.
- [19] T.V. Sokolova, I.R. Kozolva, K. Derko, A.V. Kiiki, *Izv. Akad. Nauk. S.S.S.R. Neorg. Mat.* 9 (1968) 611.
- [20] P. Zoltowski, *Rev. Int. Hautes. Temper. Et. Refract.* 5 (1968) 253.